ACS Sustainable Chemistry & Engineering

Research Article

pubs.acs.org/journal/ascecg

Concurrent Production of Carbon Monoxide and Manganese(II) Oxide through the Reaction of Carbon Dioxide with Manganese

Wonhee Lee and Jae W. Lee*

Department of Chemical and Biomolecular Engineering, Korea Advanced Institute of Science and Technology (KAIST), 291 Daehak-ro, Yuseong-gu, Daejeon 305-701, Republic of Korea

Supporting Information

ABSTRACT: This study introduces the simultaneous production of manganese oxide (MnO (II)) and carbon monoxide (CO) from the reaction of carbon dioxide (CO_2) with manganese (Mn) at ambient pressures. The reaction results showed that Mn oxidation in the presence of CO_2 creates highly pure MnO (99.4 mol %) and a small portion of another manganese oxide (Mn_3O_4 (III)) with the evolution of CO. It is striking that the oxidation path of manganese under CO_2 environments is totally reverse compared to that under oxygen (O_2) environments, and it produces MnO at much lower temperature (around 700 °C) than the temperature (1700 °C) from the O_2 oxidation path. The different patterns of Mn oxidation by both CO_2 and O_2 can arise from the differences in thermodynamic stability and reactivity of CO_2 and O_2. Additionally, mass spectroscopic measurements revealed that CO generation originates from the CO_2 reduction. Above 700 °C, more CO was produced by the reverse Boudouard reaction occurring between the carbon deposited on the manganese oxide surface and CO_2. This Mn−CO_2 reaction system provides an opportunity for producing more valuable products such as MnO and CO by utilizing the greenhouse gas.

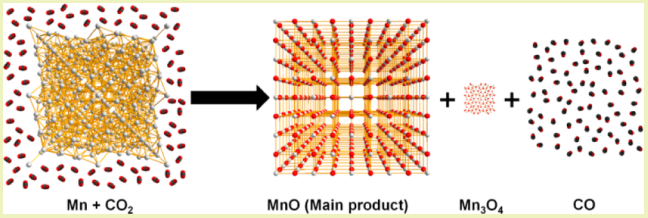

KEYWORDS: *Carbon dioxide (CO_2), Carbon monoxide (CO), Manganese (Mn), Manganese(II) oxide (MnO), Carbon dioxide (CO_2) chemical conversion*

INTRODUCTION

Modern society requires a substantial consumption of energy to maintain the quality of human life and operation of industrial infrastructure to which we are accustomed. The primary energy resources to provide the world's energy requirements include various fossil fuels such as petroleum, coal, and natural gas.[1] Only a small portion of the energy supply is provided by hydroelectric, geothermal, and other renewable energies.[1] Even though diverse sustainable energies, such as solar, biomass, wind, tides, ocean waves, and ocean thermal power, have been widely explored, the capital cost of renewable energy technologies is high in comparison with that of conventional fossil fuel plants.[1] Hence, the fossil fuel demand and consumption of the world has kept growing as the population of the world increases and developing countries are industrialized.

CO_2 is a common final product as a result of hydrocarbon combustion, mainly in vehicles and chemical and power plants, which creates the man-made greenhouse effect, leading to the gradual increase in the temperature of Earth. The temperature rise of Earth's surface may bring about several serious problems of climate change and sea level rise that could profoundly influence human life and ecology. For this reason, CO_2-related technologies including gas separation,[2−11] geological storage,[12,13] and conversion to useful chemical products[14−20] have been widely investigated to reduce the amount of greenhouse gas emissions and to prevent global warming. Among them, CO_2 conversion has generated great interest from the aspects of the reutilization of greenhouse gas and creation of a novel industrial carbon cycle, that is, the carbon cycle realized in industry rather than in nature. Here, the industrial carbon cycle is the cyclic consecutive process consisting of the carbon-based compound-consuming processes generating CO_2 (i.e., oxidation of fuels or general chemical reactions), CO_2 capturing processes, and CO_2 conversion processes to create valuable products, such as various hydrocarbons, oxygenates, and synthetic gas. The diversity of the CO_2 conversion process facilitates the variety of the industrial carbon cycle, saving energy sources and reducing environmental impact. However, CO_2 conversion has been considered as one of the most challenging topics for scientists and engineers because CO_2 is featured by its thermodynamic stability, resulting in the requirement of a substantial amount of energy to realize the conversion process. Accordingly, researchers have attempted a variety of methods including chemical,[14−18] photochemical,[19] and biological[20] CO_2 conversion processes. In particular, the thermochemical cycles using metal/metal oxide redox reactions, especially the Zn/ZnO redox couple, have been extensively studied to produce carbon monoxide (CO) and hydrogen (H_2) by CO_2 and H_2O

Received: March 11, 2014
Revised: May 7, 2014
Published: May 8, 2014

splitting.[17,18] This process is divided into two steps: (1) CO/H_2 production step by the reaction of Zn with CO_2/H_2O and (2) ZnO recycle step using a solar reactor to regenerate Zn.[17,18] However, ZnO reduction requires an extremely large amount of energy, higher than 400 kJ mol^{-1} of energy input with the approximate operation temperature of 1900 °C, and thus, the process has to be accompanied by a highly advanced solar energy concentrating technology.[17,18]

This work proposes another method of CO_2 conversion by following the concept of the reaction of a metal in the presence of CO_2 without using a solar reactor. The strategy can be the creation of a useful material through the CO_2 reduction process by which the resultant product must be an oxidized form of the reducing agent. We will demonstrate that CO_2 is reduced to CO using manganese (Mn) as a reducing agent that is simultaneously oxidized to manganese(II) oxide (MnO) to realize the economic feasibility. The thermal reduction of MnO is also highly endothermic as in the case of ZnO, which can be anticipated from the fact that two sequential thermal reductions of Mn_2O_3 to Mn_3O_4 and Mn_3O_4 to MnO with the operation temperature of above 1562 °C require activation energies around 300 kJ mol^{-1} and 400 kJ mol^{-1}, respectively.[21] The process proposed in this study does not require this thermal reduction because MnO is not further thermally treated but can be directly applied for various usages as a final product. This metal oxide can be used as an anode material of a Li-ion battery,[22] a catalyst for allyl alcohol production, a component of fertilizer, a food additive, and so on. Additionally, the other valuable product, CO, is widely utilized as a primary component for the synthesis of various useful chemicals including aldehydes, methanol, phosgene, and so on. Campbell et al. studied the reaction of CO_2 with Mn and focused on the CO_2 conversion rate up to 500 °C.[23] However, we will investigate not only the reaction kinetics of Mn with CO_2 by thermal gravimetric analysis (TGA) but also the crystal structures of the products by powder X-ray diffraction (PXRD) that are synthesized in a small-scale tube reactor, as well as CO production from the CO_2 reduction by mass spectroscopy (MS). We will contrast the difference in oxidation mechanisms of Mn in the presence of O_2 and CO_2.

EXPERIMENTAL SECTION

Reagents. Mn (powder, −325 mesh) with a purity of ≥99% was purchased from Sigma-Aldrich, and CO_2 with a purity of >99.8% was supplied by Deokyang Co., Ltd. All of the chemicals were used as received without further purification.

Thermal Analyses of the Reaction of Mn with CO_2. The reaction of Mn in the presence of CO_2 was carried out using a thermal gravity analyzer (Setaram Instrumentation) with a CO_2 flow rate of 80 cm^3 min^{-1}. About 11 mg of Mn powder was loaded in an alumina crucible, and then the sample and reference crucibles were heated to 500, 700, and 900 °C from room temperature. The heating rate was 5 °C min^{-1} for all of the target temperatures. After reaching each target temperature, the temperature was maintained for 3 h. Then, the crucibles were cooled to room temperature.

Sample Preparation. About 1 g of Mn powder was loaded in an alumina crucible boat, and then the boat was placed in a horizontal quartz tube that was mounted in a furnace (GSL1100X, MTI Co.). CO_2 was supplied into the quartz tube with a flow rate of 80 cm^3 min^{-1} during the experiments. The quartz tube was heated to 500, 700, and 900 °C from room temperature with a heating rate of 5 °C min^{-1}, followed by maintaining at the specified temperatures for 3 h, respectively, and then finally cooled to room temperature. After the reaction of Mn with CO_2, the metal powder samples were agglomerated to each other and became plate-like shapes because the Mn atoms were bound to O atoms provided by CO_2. The resultant product was turned upside down, and the same experiment was performed to complete the reaction of the unreacted Mn with CO_2. Photos were taken of all of the samples in the alumina boats whenever the reactions were finished. The compositions of the final products synthesized at 700 and 900 °C were determined by the material balance from the mass change of the samples before and after the reaction. The actual weight of the Mn was calculated by multiplying the initial weight of the Mn powder by 0.99 to consider the purity of the reagent.

Sample Characterization and Measurement. The powder X-ray Diffraction (PXRD) patterns of the finely ground final products synthesized at different temperatures were recorded on a Rigaku D/MAX-RB (12 KW). The light source was graphite-monochromatized Cu $K\alpha_1$ radiation with a wavelength of 1.5406 Å. The voltage and current of the generator were 40 kV and 100 mA, respectively. The PXRD patterns were obtained in a continuous scan mode with a scan speed of 4° min^{-1} for 2θ = 10°∼80°.

Elemental analysis (EA) of the final products was performed using the elemental analyzer (FLASH 2000 series) to determine the amount of carbon deposited in the solid products.

The mass spectrometer (QMS 200, Pfeiffer Vacuum) was connected to the outlet of the quartz tube for the confirmation of CO evolution during the reaction at each target temperature.

RESULTS AND DISCUSSION

Mn is one of the potent candidate metals that can react with CO_2 to yield CO as in the case of Zn/ZnO and FeO/Fe_3O_4 redox couples.[17,18] It has a high possibility of simultaneously producing valuable forms of manganese oxides with CO by the same reaction between CO_2 and Mn. Considering the various useful applications of manganese oxides, it is very attractive to utilize this process for the production of the unknown oxides. Figure 1 shows TGA diagrams representing the weight and temperature profiles of Mn samples during the reaction with CO_2. We carried out the reaction experiments at three target temperatures, 500, 700, and 900 °C, to reveal the temperature effect on the reaction kinetics. The red and blue lines represent the temperature and weight, respectively. All three cases exhibit that the weights of the samples increase as the temperature rises, indicating that Mn oxidation by CO_2 forms certain manganese oxides. The weights in the three samples start suddenly increasing after about 70 min at 375 °C, but the reaction kinetics at each temperature is quite different. The reaction of the sample synthesized at 500 °C is not completely finished because the weight of the sample keeps increasing despite the 3 h of holding time at 500 °C. On the other hand, the weight increase of the product obtained at 700 °C is almost converged after maintaining the target temperature for 3 h. In the case of the sample synthesized at 900 °C, the reaction is entirely terminated before reaching the target temperature. These TGA results indicate that the Mn oxidation rate by CO_2 becomes faster as the temperature increases, and 700 °C could be enough to complete the reaction for 3 h.

Even though it is revealed that Mn can be oxidized in the presence of CO_2 from the TGA measurement, it is necessary to further disclose what types of manganese oxides are produced after the reaction. Because manganese oxides possess several crystal forms, such as MnO, Mn_3O_4, Mn_2O_3, and MnO_2, the crystal structures of the products need to be identified by PXRD. To prepare the samples for obtaining PXRD patterns, gray Mn powder is loaded into an alumina crucible boat of the furnace. After the reaction at 500 °C, under the 5 °C min^{-1} of heating rate and the 3 h of holding time, the powder sample becomes hard and brown by the reaction of Mn atoms with O

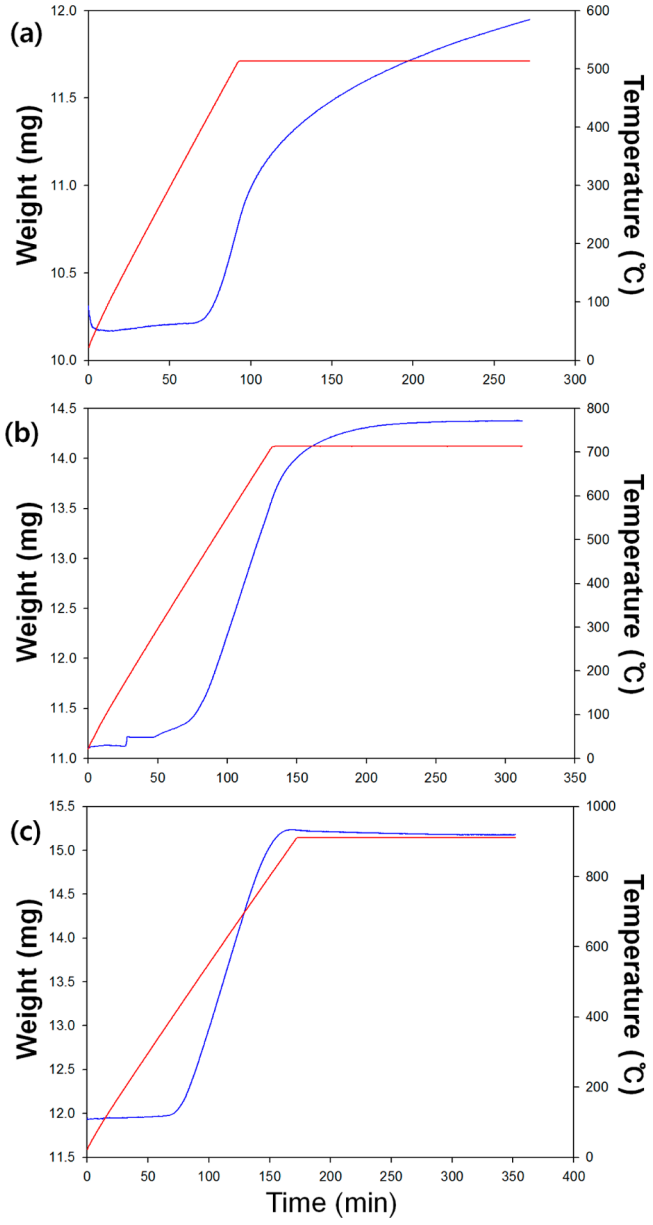

Figure 1. TGA diagrams of weight and temperature profiles for the Mn reaction with CO_2 at (a) 500 °C, (b) 700 °C, and (c) 900 °C (red lines, temperature; blue lines, weight).

atoms of CO_2 (Figure 2a). It is anticipated that the lower surface of the Mn powder possesses less opportunities to contact with CO_2 to form manganese oxides. Thus, the resultant sample is placed upside down, and the lower surface was still gray (Figure 2b), implying that unreacted Mn is present even after the reaction.

The weight increases before and after the reactions also support the existence of unreacted Mn as shown in Figure 3. If the Mn powder is fully converted into MnO, the weight must be increased as high as 29.12 wt %. However, the weight of the sample is increased only by 15.57 wt % at 500 °C. The weight variations of the samples after the reactions at 700 and 900 °C under the same heating rate and holding time do not also reach the stoichiometric weight percentage (29.12 wt %) and are just increased up to 28.05 and 28.39 wt %, respectively. Accordingly, all of the samples are reacted again under the same conditions with their lower surfaces upward to be exposed

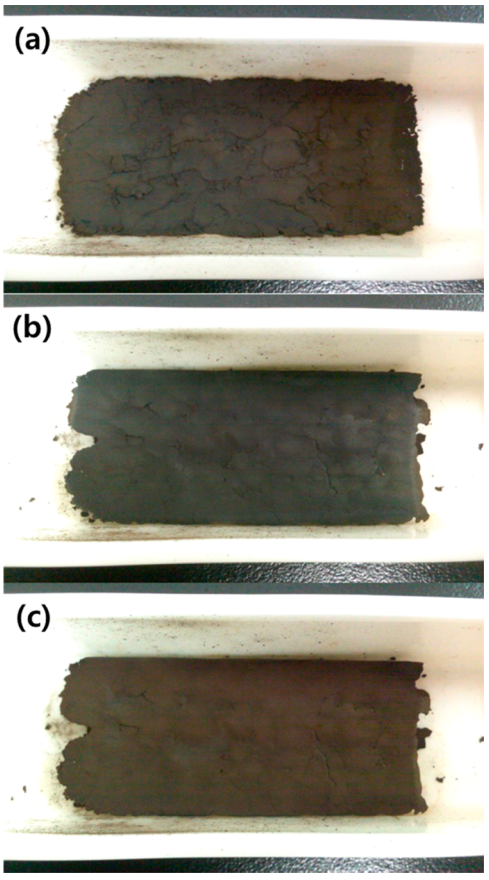

Figure 2. Photos of the sample synthesized at 500 °C: (a) after the first reaction, (b) the samples turned upside down, and (c) the final products after the second reaction.

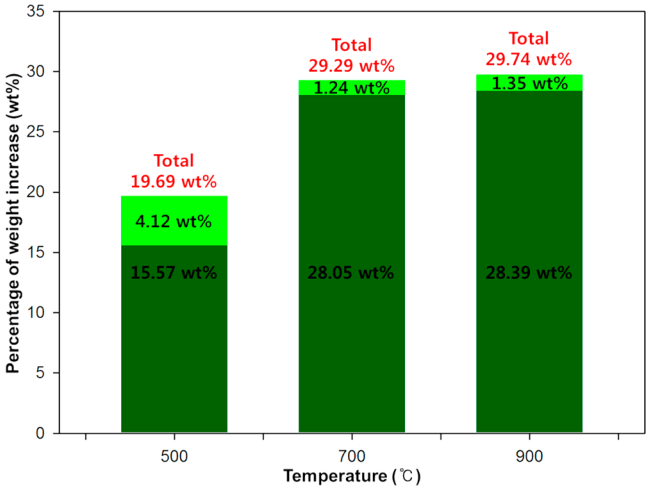

Figure 3. Percentage of weight increase after first (green) and second (light green) reactions.

to CO_2 gas. Figure 2 c shows the surface of the sample produced at 500 °C after the second reaction, representing that the gray surface is changed to brown, which means that more Mn is reacted with CO_2. The photos of other samples after the reactions are shown in Figure S1 of the Supporting Information. The weight of the final products at 500, 700, and 900 °C are further increased by 4.12, 1.23, and 1.35 wt %, and the total amounts of weight increases are 19.69, 29.29, and

dx.doi.org/10.1021/sc500179r | ACS Sustainable Chem. Eng. 2014, 2, 1503−1509

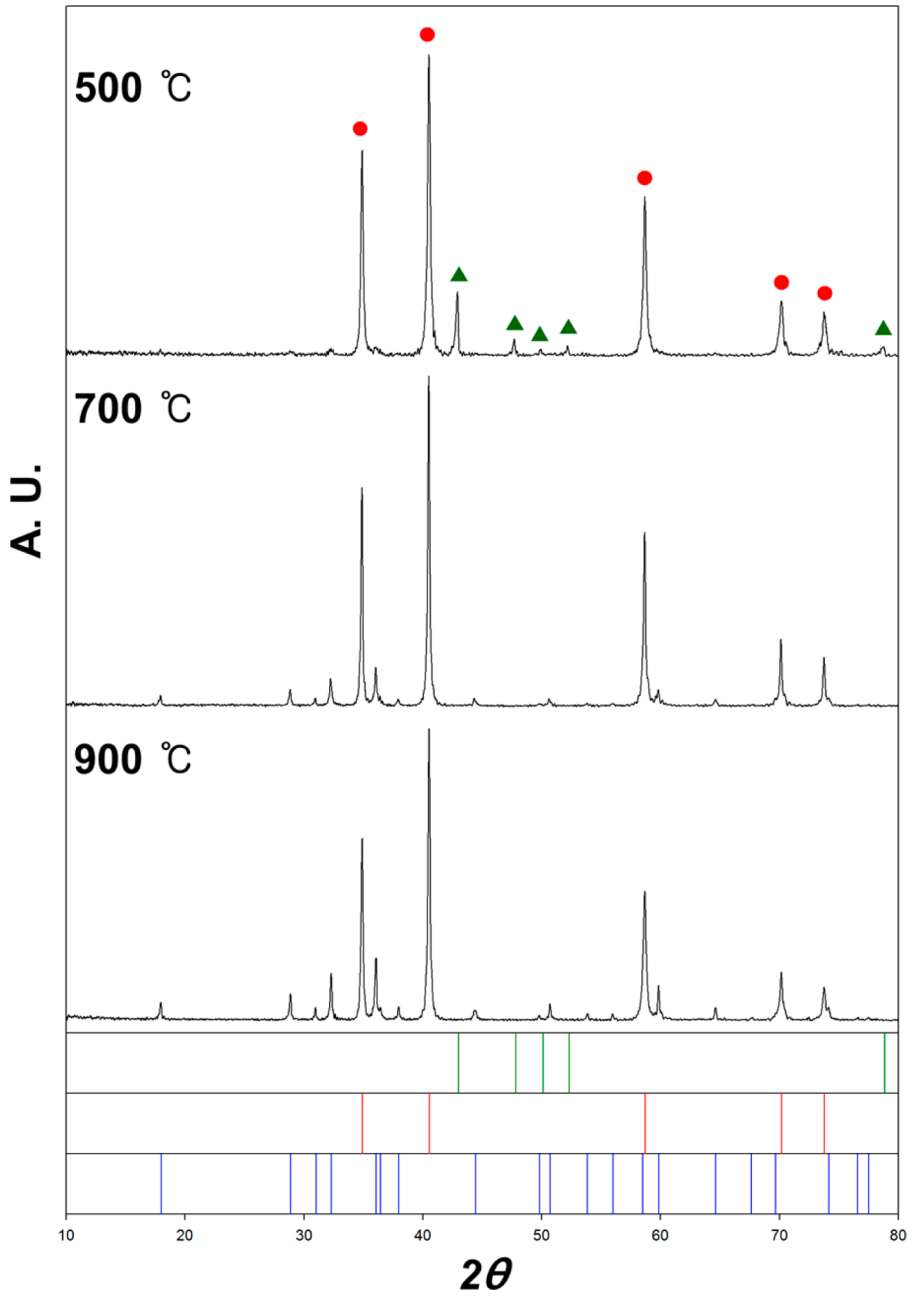

Figure 4. XRD patterns of the final products synthesized at 500, 700, and 900 °C (green lines and triangles, Mn; red lines and circles; MnO; blue lines; Mn_3O_4).

29.74 wt %, respectively. From this information, there still remains a considerable amount of unreacted Mn in the final sample produced at 500 °C even after the two steps of reactions with CO_2. However, the weight increases of the other two samples synthesized at 700 and 900 °C exceed the stoichiometric weight percentage, 29.12 wt %, which means that other forms of manganese oxides or other materials exist in the samples. Therefore, it is necessary to determine the crystal structures of the components using PXRD to disclose their identities.

Figure 4 shows the PXRD patterns of the final products from the two steps of the Mn oxidation by CO_2, and the following information can be obtained from this measurement. First of all, MnO (indicated by red lines and circles) is the main product in all of the three samples reacted at 500, 700, and 900 °C, and thus, this study focuses on the production of high purity of MnO. The product synthesized at 500 °C also contains unreacted Mn (indicated by green lines and triangles) and a very small amount of Mn_3O_4 (indicated by blue lines). The presence of the unreacted Mn in this sample corresponds with the result obtained from the low increment of the sample weight in the furnace experiment (Figure 3). Consequently, the Mn oxidation by CO_2 at 500 °C is inappropriate to produce high purity of MnO. In the PXRD pattern (Figure 4) of the sample reacted at 700 °C, only peaks of two components, MnO and Mn_3O_4, exist. The peak intensity of Mn_3O_4 slightly increases, while that of the unreacted Mn completely disappears. The sample synthesized at 900 °C also contains only MnO and Mn_3O_4, and more Mn_3O_4 is produced under this condition in comparison with the amount of Mn_3O_4 in the

dx.doi.org/10.1021/sc500179r | ACS Sustainable Chem. Eng. 2014, 2, 1503−1509

other two samples. This result indicates that Mn is more oxidized to form Mn_3O_4 as the temperature rises.

At this stage, it is important to determine the composition of the samples to discover the experimental conditions where the high purity of MnO is achieved. Above all, the EA is performed to find out the small amount of carbon in the samples that could be deposited on the surface of the manganese oxides because CO, which is a product resulting from the overall process, possibly creates carbon by the Boudouard reaction ($2CO \rightarrow CO_2 + C$).[24] The EA result tells us that the sample produced at 500 °C possesses 0.4 wt % of carbon content, while the other samples contain no carbon, indicating that only MnO and Mn_3O_4 exist in the samples synthesized at 700 and 900 °C.

Then, the compositions of the final products after the two reactions are computed by material balances of Mn and O elements. As a result of the calculations, the sample produced at 700 °C is composed of 99.4 mol % (98.2 wt %) of MnO and 0.6 mol % (1.8 wt %) of Mn_3O_4, while that produced at 900 °C consists of 98.0 mol % (94.0 wt %) of MnO and 2.0 mol % (6.0 wt %) of Mn_3O_4. (For the calculation procedure, please refer to the Supporting Information). The composition of the sample synthesized at 500 °C cannot be evaluated by this method because the existence of the unreacted Mn is an unknown. According to this calculation, the reaction temperature of 700 °C is a very appropriate condition to obtain the high purity of MnO through Mn oxidation by CO_2. It is noticeable that the carbon content is only discovered in the sample reacted at 500 °C. This phenomenon can be understood from the CO evolution trend depending on the reaction temperature because the Boudouard reaction equilibrium can shift to the reverse direction of CO generation at higher temperatures than 500 °C.

In this study, not only the MnO production but also the CO evolution from CO_2 reduction is an important objective because the overall process includes the CO_2 conversion that makes it possible to utilize the greenhouse gas. We measured the variation of the amount of CO_2 and CO during the reactions at different target temperatures using a mass spectrometer (MS), and the results are shown in Figure 5. The MS measurement well represents that the CO evolution trend follows the CO_2 reduction tendency depending on the temperature. The interesting point in this figure is the existence of other peaks indicated by the arrows in Figure 5 that appear only in the samples reacted at 700 and 900 °C, which could originate from a different CO evolution mechanism at high temperatures other than the CO_2 reduction from the reaction with Mn. This phenomenon can be considered in relation to the EA result. Even though the carbon deposited in the sample synthesized at 500 °C is also unavoidably created in the other samples produced at 700 and 900 °C, these samples at the two high temperatures do not contain any carbon. Hence, the carbon created at lower temperatures by the Boudouard reaction disappears at higher temperatures than 500 °C. The Boudouard reaction is basically the chemical equilibrium redox reaction between CO and CO_2, which means that the equilibrium composition of the mixture can be influenced by the temperature.[24] As the temperature rises, the equilibrium shifts to the reverse Boudouard reaction ($CO_2 + C \rightarrow 2CO$),[24] implying that more CO is generated by the reaction of CO_2 with the carbon already deposited on the surface of the products. This is the reason why the carbon cannot be discovered in the samples synthesized at 700 and 900 °C.

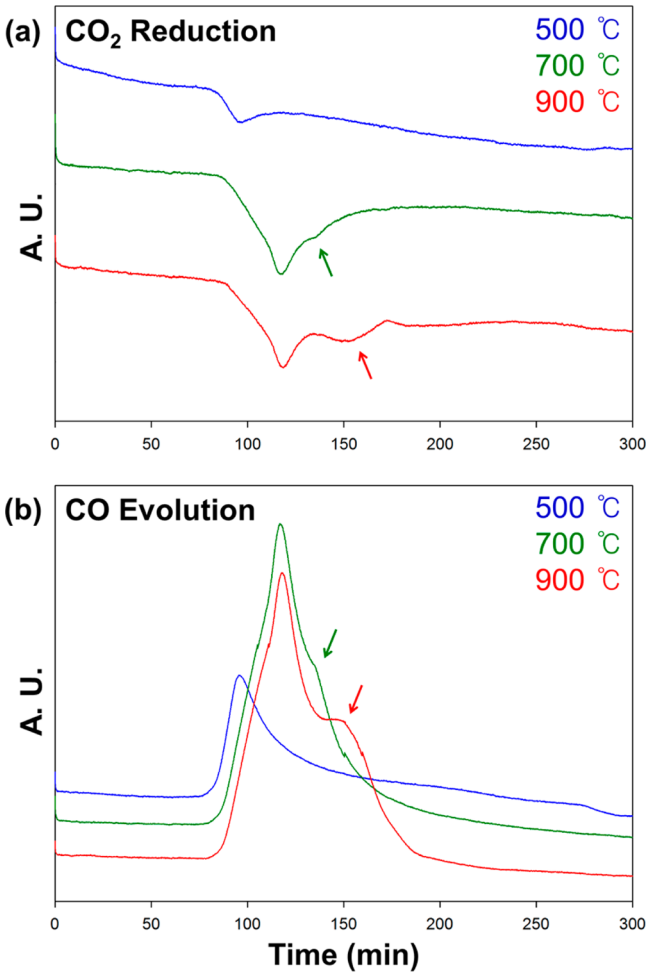

Figure 5. CO_2 reduction and CO evolution measured by MS at 500 °C (blue), 700 °C (green), and 900 °C (red).

Finally, it is also interesting to note that other manganese oxides, such as Mn_2O_3, and MnO_2, cannot be found in the final products. We need to consider the oxidation circumstances for a better understanding of the oxidation mechanism of Mn in the presence of CO_2. Scheme 1 shows various manganese

Scheme 1. Mn oxidation in the Presence of (a) O_2 Depending on the Temperature and (b) CO_2

(a) $Mn + O_2 \longrightarrow MnO_2 \xrightarrow{500\ ℃} Mn_2O_3 \xrightarrow{900\ ℃} Mn_3O_4 \xrightarrow{1700\ ℃} MnO$

(b) $(x+3y)Mn + (x+4y)CO_2 \xrightarrow{700\ ℃} xMnO\ (Main) + yMn_3O_4 + (x+4y)CO$

oxides formed with O_2 depending on the temperature[25] and with CO_2. The Mn oxidation in O_2 first creates MnO_2, which is the most oxidized crystal of Mn, below 500 °C and then forms Mn_2O_3, Mn_3O_4, and MnO up to 1700 °C, in the order of high to low oxidation number as the temperature increases.[25] On the other hand, Mn is oxidized by CO_2 to yield MnO as a main product and a small amount of Mn_3O_4 at temperatures as low as 700 °C, which is a large contrast to 1700 °C from the O_2 oxidation path to produce MnO.

The difference in the oxidation sequence of Mn can be considered to originate from several reasons. Above all, the thermodynamic stability of the two molecules, CO_2 and O_2, is one of the factors; the Gibbs free energy of formation of CO_2 is -394.36 kJ mol^{-1}, whereas that of O_2 is 0 kJ mol^{-1}.[26]

dx.doi.org/10.1021/sc500179r | ACS Sustainable Chem. Eng. 2014, 2, 1503−1509

Accordingly, the CO_2-based oxidation has to be realized under the condition of higher temperature. The existence of unreacted Mn after the reaction at 500 °C implies that more energy is required to fully activate CO_2 for the reaction with Mn, and the reaction temperature is not proper to create the highly oxidized form of Mn. Because MnO_2 is thermally decomposed at 535 °C, the oxide phase cannot appear in the samples synthesized above the decomposition temperature. This is the reason why Mn is oxidized to form MnO_2 below 500 °C by O_2 rather than CO_2. The absence of Mn_2O_3 (decomposition temperature: 940 °C) under CO_2 environments can be explained by another factor, which is the lower reactivity of CO_2 toward Mn than O_2. Figure 6 shows a simplified illustration of the Mn oxidation mechanism in the presence of CO_2 by contrasting with the oxidation path under O_2 on the basis of the explanation of a previous work.[27] O_2 or CO_2 molecules must approach the Mn crystal and then be adsorbed on the metal surface. The adsorbed molecules are split into two O atoms or a CO molecule and O atom. The highly electronegative O atoms adsorbed on the Mn surface attract the electrons from the Mn crystal to be chemisorbed and then eventually form a manganese oxide lattice. However, the CO molecule cannot be provided with electrons from the Mn surface and does not undergo the ionization stage because the O atom is covalently bonded with the C atom to form a triple bond and already attracts some portion of electrons from the C atom. As a result, CO molecules tend to be desorbed from the Mn surface and fly away as a gaseous phase. From this consideration, more O atoms can be easily incorporated into the manganese oxide lattice in the presence of O_2 rather than CO_2. Therefore, unlike the oxidation in O_2, Mn oxidation by CO_2 forms mainly MnO at much lower temperature, which is the lowest oxidized form of manganese oxides, and creates a small portion of Mn_3O_4 rather than more highly oxidized phases, MnO_2 and Mn_2O_3.

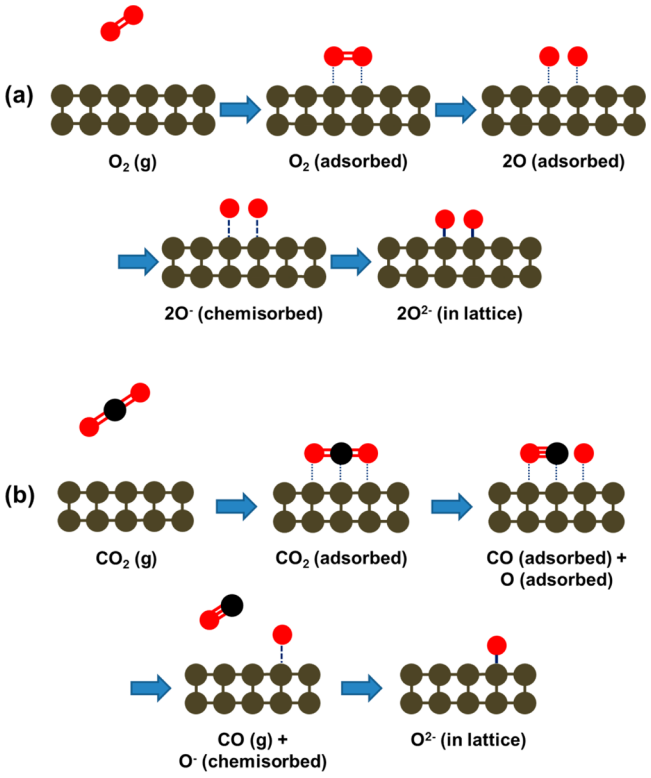

Figure 6. Simplified illustration of oxidation mechanism of Mn in the presence of (a) O_2 and (b) CO_2.

The total production of Mn in 2009 was 33.5 million tons,[28] and we cannot find the statistical data of the amount of MnO consumption. If we assume 5% (1.7 million tons of Mn) of the total production of Mn is used for the production of MnO, our proposed process can consume about 1.4 million tons of CO_2 to produce 2.2 million tons of MnO and 0.87 million ton of CO.

CONCLUSION

The process investigated in this study is quite simple and simultaneously produces valuable chemicals such as pure MnO and CO. MnO is commercially prepared by the reaction of manganese dioxide (MnO_2) with H_2, CO, or methane (CH_4). The commercially available MnO production system must consume natural gas to synthesize the reducing agents H_2 or CO by CH_4 reforming and fossil fuels to increase the reaction temperature. The novel process that we propose does not use CH_4 or the reforming-based products (syngas, H_2, CO) to reduce MnO_2. Rather, we utilize CO_2 to oxidize Mn to MnO at much lower temperature than the oxidation path under O_2 environments. Another advantage of this process is that the amount of the final product is about 1.29 times more mass than that of the reactant because MnO can be obtained by the reaction of Mn with O originating from CO_2. Additionally, the process proposed in this study can be economically feasible because MnO is generally more expensive than Mn. This study provides the co-production of MnO and CO through CO_2 reduction and the basic information on Mn oxidation mechanism in the presence of CO_2. On the basis of this approach, the process will be further optimized for more refined MnO production and for more efficient energy consumption of the process.

ASSOCIATED CONTENT

Supporting Information

Material balance calculation procedures and visual observations of reacted solid phases of manganese oxides with CO_2. This material is available free of charge via the Internet at http://pubs.acs.org.

AUTHOR INFORMATION

Corresponding Author

*E-mail: jaewlee@kaist.ac.kr.

Notes

The authors declare no competing financial interest.

ACKNOWLEDGMENTS

The authors are grateful for the financial support from the Korea CCS R & D Center funded by the Ministry of Science, ICT, and Future Planning (NRF-2013M1MA8A1040703).

REFERENCES

(1) Fay, J. A.; Golomb, D. *Energy and the Environment*; Oxford University Press: New York, 2002.

(2) Rochelle, G. T. Amine scrubbing for CO_2 capture. *Science* **2009**, *325* (5948), 1652−1654.

(3) Neveux, T.; Le Moullec, Y.; Corriou, J. P.; Favre, E. Modeling CO_2 capture in amine solvents: Prediction of performance and insights on limiting phenomena. *Ind. Eng. Chem. Res.* **2013**, *52* (11), 4266−4279.

(4) Brunetti, A.; Scura, F.; Barbieri, G.; Drioli, E. Membrane technologies for CO_2 separation. *J. Membr. Sci.* **2010**, *359* (1−2), 115−125.
(5) Atsonios, K.; Panopoulos, K. D.; Doukelis, A.; Koumanakos, A.; Kakaras, E. Cryogenic method for H_2 and CH_4 recovery from a rich CO_2 stream in pre-combustion carbon capture and storage schemes. *Energy* **2013**, *53*, 106−113.
(6) Millward, A. R.; Yaghi, O. M. Metal-organic frameworks with exceptionally high capacity for storage of carbon dioxide at room temperature. *J. Am. Chem. Soc.* **2005**, *127* (51), 17998−17999.
(7) Wang, B.; Cote, A. P.; Furukawa, H.; O'Keeffe, M.; Yaghi, O. M. Colossal cages in zeolitic imidazolate frameworks as selective carbon dioxide reservoirs. *Nature* **2008**, *453* (7192), 207−U6.
(8) Patel, H. A.; Je, S. H.; Park, J.; Chen, D. P.; Jung, Y.; Yavuz, C. T.; Coskun, A. Unprecedented high-temperature CO_2 selectivity in N_2-phobic nanoporous covalent organic polymers. *Nat. Commun.* **2013**, DOI: 10.1038/ncomms2359.
(9) Kang, S. P.; Lee, H. Recovery of CO_2 from flue gas using gas hydrate: Thermodynamic verification through phase equilibrium measurements. *Environ. Sci. Technol.* **2000**, *34* (20), 4397−4400.
(10) Seo, Y.; Kang, S.-P. Enhancing CO_2 separation for pre-combustion capture with hydrate formation in silica gel pore structure. *Chem. Eng. J.* **2010**, *161* (1−2), 308−312.
(11) Kang, S.-P.; Lee, J.; Seo, Y. Pre-combustion capture of CO_2 by gas hydrate formation in silica gel pore structure. *Chem. Eng. J.* **2013**, *218*, 126−132.
(12) Schrag, D. P. Storage of carbon dioxide in offshore sediments. *Science* **2009**, *325* (5948), 1658−1659.
(13) Michael, K.; Golab, A.; Shulakova, V.; Ennis-King, J.; Allinson, G.; Sharma, S.; Aiken, T. Geological storage of CO_2 in saline aquifers − A review of the experience from existing storage operations. *Int. J. Greenhouse Gas Control* **2010**, *4* (4), 659−667.
(14) Zhang, J.; Lee, J. W. Production of boron-doped porous carbon by the reaction of carbon dioxide with sodium borohydride at atmospheric pressure. *Carbon* **2013**, *53*, 216−221.
(15) Zhang, J.; Byeon, A.; Lee, J. W. Boron-doped electrocatalysts derived from carbon dioxide. *J. Mater. Chem. A* **2013**, *1* (30), 8665−8671.
(16) Byeon, A.; Lee, J. W. Electrocatalytic activity of BN codoped graphene oxide derived from carbon dioxide. *J. Phys. Chem. C* **2013**, *117* (46), 24167−24173.
(17) Loutzenhiser, P. G.; Meier, A.; Steinfeld, A. Review of the two-step H_2O/CO_2-splitting solar thermochemical cycle based on Zn/ZnO redox reactions. *Materials* **2010**, *3* (11), 4922−4938.
(18) Roeb, M.; Neises, M.; Monnerie, N.; Call, F.; Simon, H.; Sattler, C.; Schmücker, M.; Pitz-Paal, R. Materials-related aspects of thermochemical water and carbon dioxide splitting: A review. *Materials* **2012**, *5* (11), 2015−2054.
(19) Khenkin, A. M.; Efremenko, I.; Weiner, L.; Martin, J. M. L.; Neumann, R. Photochemical reduction of carbon dioxide catalyzed by a ruthenium-substituted polyoxometalate. *Chem. − Eur. J.* **2010**, *16* (4), 1356−1364.
(20) Shi, J.; Wang, X.; Jiang, Z.; Liang, Y.; Zhu, Y.; Zhang, C. Constructing spatially separated multienzyme system through bioadhesion-assisted bio-inspired mineralization for efficient carbon dioxide conversion. *Bioresour. Technol.* **2012**, *118*, 359−366.
(21) Alonso, E.; Hutter, C.; Romero, M.; Steinfeld, A.; Gonzalez-Aguilar, J. Kinetics of Mn_2O_3-Mn_3O_4 and Mn_3O_4-MnO redox reactions performed under concentrated thermal radiative flux. *Energy Fuels* **2013**, *27* (8), 4884−4890.
(22) Liu, X.; Chen, C.; Zhao, Y.; Jia, B. A review on the synthesis of manganese oxide nanomaterials and their applications on lithium-ion batteries. *J. Nanomater.* **2013**, *2013*, 7.
(23) Campbell, A. N.; Brown, E. A. The action of carbon dioxide and of carbon monoxide on manganese. *J. Am. Chem. Soc.* **1938**, *60* (12), 3055−3060.
(24) Wiberg, E.; Wiberg, N.; Holleman, A. F. *Inorganic Chemistry*, 1st English ed.; Academic Press: San Diego, 2001.
(25) Stobbe, E. R.; de Boer, B. A.; Geus, J. W. The reduction and oxidation behaviour of manganese oxides. *Catal. Today* **1999**, *47* (1−4), 161−167.
(26) Atkins, P. W.; De Paula, J. *Atkins' Physical Chemistry*, 8th ed.; Oxford University Press: Oxford, U.K., 2006.
(27) Birks, N.; Meier, G. H.; Pettit, F. S. *Introduction to the High-Temperature Oxidation of Metals*, 2nd ed.; Cambridge University Press: Cambridge, U.K., 2006.
(28) Brown, T. J.; Bide, T.; Walters, A. S.; Idoine, N. E.; Shaw, R. A.; Hannts, S. D.; Lusty, P. A. J.; Kendall, R. *World Mineral Production 2005−2009*; British Geological Survey; Keyworth, Nottingham, 2011.